Supplementary Materials and Methods

Immunofluorescence

Paraffin-embedded tissue sections were deparaffinized in xylene and rehydrated using a graded series of ethanol. After antigen retrieval in sodium citrate buffer (10 mM, pH 6.0) and blocking by goat serum, immunofluorescence staining for all slides was performed with a primary antibody (mouse monoclonal anti-8-OHdG antibody, ab48508, 1:200, Abcam, Cambridge, MA; rabbit monoclonal anti-SIRT3 antibody, #2627, 1:200, Cell Signaling Technology, Beverly, MA; rabbit monoclonal anti-SOD2 (acetyl K68) antibody, ab137037,1:200, Abcam; rabbit polyclonal anti-PGC1α antibody, ab54481, 1:200, Abcam). Primary antibody Melan-A (mouse monoclonal anti-Melan A antibody, ab187369, 1:300, Abcam) was used to co-stain for melanocytes. All the primary antibodies were incubated overnight at 4 °C, followed by 1 h incubation with appropriate secondary antibodies (Alexa Fluor 488 anti-rabbit IgG, #4412, 1:200, Cell Signaling Technology or Alexa Fluor 594 anti-mouse IgG, #8890, 1:200, Cell Signaling Technology). Nuclei were counterstained with DAPI (Dako, Glostrup, Denmark). Fluorescence was analyzed by confocal laser scanning microscopy (FV-1000, Olympus, Tokyo, Japan). For immunofluorescence of cultured cells, NHEMs, PIG1 cells and PIG3V cells were first seeded on coverslips in a 24-well plate and allowed to adhere before staining. After fixed with 4 % paraformaldehyde for 10 min, and permeabilized with 0.5% Triton X-100 for 10 min, cells were stained using rabbit monoclonal anti-SIRT3 antibody (#2627, 1:200, Cell Signaling Technology) overnight at 4 °C, followed by the Alexa Fluor 488 anti-rabbit IgG (#4412, 1:200, Cell Signaling Technology) at room temperature for 1 h. Nuclei were stained with DAPI (Dako) and subsequently analyzed by confocal laser scanning microscopy (FV-1000).

RNA interference

SiRNAs specifically targeting SIRT3 and OPA1 were purchased from GenePharma (Shanghai, China) using the following sequences: si-SIRT3-sense: 5'-GGAAAGCCUAGUGGAGCUUTT-3', si-SIRT3-antisense: 5'-AAGCUCCACUAGGCUUUCCTT-3, si-OPA1-sense: 5'-GCUUUAUGACAGAACCGAATT-3', si-OPA1-antisense: 5'-UUCGGUUCUGUCAUAAAGCGG-3'. Cultured cells were seeded at 30% ~ 40% confluence in

six-well plates or cell culture bottle overnight before transfection, and then transfected with siRNA using Lipo3000 transfection reagent (Invitrogen) according to the manufacturer's instructions.

Plasmid construction and transfection

For overexpressing SIRT3 and OPA1, the full-length cDNA of Human SIRT3 and short form of OPA1 were cloned into pcDNA 3.1 vector and GV141 vector, respectively (Genechem, Shanghai, China). The SIRT3 plasmid and OPA1 plasmid were transfected into PIG3V and PIG1 cells using Lipo3000 transfection reagent (Invitrogen).

Quantitative real-time PCR

Total RNA from cultured cells was extracted using Trizol Reagent (Invitrogen). The synthesis of cDNA was performed using First Strand cDNA Synthesis Kit (Takara, Tokyo, Japan) according to the manufacturer's protocol. The sequences of primers for the quantitative real-time PCR (qRT - PCR) in this study are as follows: SIRT3-sense: 5'-AGCCCTCTTCATGTTCCGAAGTGT-3', SIRT3-antisense:5'-TCATGTCAACACCTGCAGTCCCTT-3', PGC1α-sense: 5'-GTAAATCTGCGGGATGATGG-3', PGC1α-antisense: 5'-AATTGCTTGCGTCCACAAA-3', β-Actin-sense:5'- TCATGAAGTGTGACGTGGACATC-3', β-Actin-antisense: 5'-CAGGAGGAGCAATGATCTTGATCT-3'. qRT - PCR was conducted using the SYBR Premix Ex Taq II (Takara) with the iQ5 PCR Detection System (Bio-Rad, Hercules, CA).

Cell viability

Cell viability was determined by the Cell Counting Kit-8 assay (SeaBioTech, Shanghai, China) according to the manufacturer's instructions. Briefly, cells were inoculated into 96-well plates. After experimental treatment, 90 μl of medium and 10 μl of Counting Kit-8 solution were added to each well. The cells were then incubated at 37 °C for 2 h. After incubation, optical density was measured at 450 nm by the Model 680 Microplate Reader (Bio-Rad, Hercules, CA).
The results are expressed as a percentage of the control. The experiment was performed in triplicate.

Measurement of ATP levels

The level of ATP in melanocytes was measured by the ATP Bioluminescence Assay Kit (S0026, Beyotime, Shanghai, China). Briefly, cells were collected after experimental treatment and lysed with a lysis buffer, followed by centrifugation at 12,000 g for 5 mins at 4 ℃. Finally, the level of ATP was measured by mixing 50 μl of the supernatant with 50 μl of luciferase reagent, which catalyzed the light production from ATP and luciferin. The emitted light was linearly related to the ATP concentration and measured using a microplate reader (Model 680, Bio-Rad). The ATP level was normalized to total cellular protein.

4-Hydroxyneonal (4-HNE) assay

The experiment was performed according to the instructions of the Human 4-HNE (4-Hydroxynoenal) ELISA Kit (Elabscience Co., Ltd. Wuhan, China). In brief, 10^6 cells after treatment were resuspended in 150-200 ul of PBS, and disrupted by repeated freezing and thawing. The extract was centrifuged at 1500 × g for 10 min, and the supernatant was further detected. 50 μl standard substance and test samples were added to 96-well plates, followed by immediate addition with the well-conjugated biotinylated antibody to each well. Enzyme plates were then coated and incubated at 37 ℃ for 45 min. After washing, 100 μl of enzyme conjugate was added to each well and incubated for 30 min at 37 ℃. After washing, 90μl of substrate solution (TMB) was added to each well and incubate at 37 ℃ in the dark for about 15 min, following by 50μl of stop solution adding to each well. Optical density (OD 450 nm) was measured by Microplate readers.

Lipid Peroxidation MDA assay

The experiment was performed according to the instructions of the Lipid Peroxidation MDA Assay Kit (Beyotime biotechnology, Beijing, China). In brief, the treated cells were homogenized by homogenization, and the supernatant was used for the further MDA detection. 0.1 mL homogenate, standard with different concentrations and samples were added to centrifuge tube for determination. Then 0.2 mL MDA detection working fluid was added. After mixing, samples were heated at 100 ℃ for 15 min. The bath was cooled to room temperature and centrifuged at 1000 g

for 10 min at room temperature. 200 µl supernatant was added to a 96-well plate, and absorbance was measured at 532 nm using a microplate reader.

Supplementary Tables

Table S1. Patient's characteristics, vitiligo types, onset age, disease duration and disease activity

Patient no	Sex/ age	vitiligo type	onset age	disease duration (month)	Disease activity
1	F/41	Non-segmental	41	1	Active
2	M/47	Non-segmental	45	25	Active
3	M/23	Non-segmental	13	120	Active
4	F/19	Non-segmental	17	24	Active
5	F/39	Non-segmental	39	7	Active
6	M/22	Non-segmental	17	60	Active
7	F/18	Non-segmental	18	6	Active
8	M/30	Non-segmental	30	6	Active

Table S2. Healthy controls's characteristics

Healthy control no	Sex/ age
1	F/20
2	F/22
3	F/36
4	F/45
5	M/23
6	M/26
7	M/34
8	M/44

Supplementary Figure Legends

Figure S1. Increased expression and activity of SIRT3 in NHEMs and PIG1 cells under oxidative stress. (A) PIG1 cells were treated with different doses of H_2O_2 for 24 h as indicated. CCK-8 was performed to evaluate cell viability. Data represent mean ± SD (n = 3). (B) PIG3V cells were treated with different doses of H_2O_2 for 24 h as indicated. CCK-8 was performed to evaluate cell viability. Data represent mean ± SD (n = 3). (C) NHEMs were treated with different doses of H_2O_2 for 24 h as indicated. CCK-8 was performed to evaluate cell viability. Data represent mean ± SD (n = 3). (D, E) PIG1 cells were treated with different doses of H_2O_2 as indicated. The expression of SIRT3 mRNA and protein was measured by qRT-PCR and western blotting, respectively. β-Actin was detected as loading control, Data are representative of three independently performed experiments. (F) PIG1 cells were treated with 1.0 mM H_2O_2 for 1 h, 3 h, 6 h, 12 h and 24 h, respectively. The expression of SIRT3 protein was measured by Western blotting. β-Actin was detected as loading control. Data are representative of three independently performed experiments. (G) The expression of SIRT3 protein in PIG1 cells, PIG3V cells and NHEMs were measured by Western blotting. β-Actin was detected as loading control. Data are representative of three independently performed experiments. (H) The relative mRNA level of SIRT3 in NHEMs after the treatment with 1.0 mM H_2O_2 for 24 h. Data represent mean ± SD (n = 3). (I) The protein level of SIRT3 in NHEMs after the treatement with 1.0 mM H_2O_2 for 24 h. (J) Immunoflurescence staining analysis of SIRT3 in NHEMs after the treatement with H_2O_2. Scale bar = 50 μm (Magnification: 600 ×). (K) SIRT3 activity in NHEMs after H_2O_2 treatment. Data represent mean ± SD (n = 3). (L) Acetylation of SOD2 in NHEMs after 1.0 mM H_2O_2 exposure for 24 h. Mean ± SD is shown (n = 3). p value was calculated by two-tailed Student's *t*-test. $^{*}p < 0.05$, $^{**}p < 0.01$, $^{***}p < 0.001$.

Figure S2. The knockdown efficiency of SIRT3 in melanocytes. (A) The knockdown efficacy of SIRT3 in PIG1 cells. Data represent mean ± SD (n = 3). (B) The knockdown efficacy of SIRT3 in NHEMs. Data represent mean ± SD (n = 3). p value was calculated by two-tailed Student's *t*-test. $^{***}p < 0.001$.

Figure S3. SIRT3 deficiency contributes to cell apoptosis and mitochondrial dysfunction in NHEMs. (A) NHEMs transfected with si-NC or si-SIRT3 were treated with different concentrations of H_2O_2 (0, 0.5, 1.0 mM), and the cell viability was determined by CCK-8. Data represent mean ± SD (n = 3). (B) The apoptotic level of NHEMs was examined by flow cytometry assay. Bar graphs represent mean ± SD (n = 3). (C)The level of apoptosis-related proteins in NHEMs after indicated treatment was detected by immunobloting. Data are representative of three independently performed experiments (mean ± SD, n = 3). (D) The ROS level of NHEMs was examined by MitoSOX™ Red mitochondrial superoxide indicator staining. Bar graphs represent mean ± SD (n = 3). (E) Assessment of ATP level in NHEMs with treatment as indicated. Data represent mean ± SD of triplicates. (F) The mitochondrial membrane potential of NHEMs was examined by JC-1 staining. The scatter plot of the flow cytometry analysis shows the distribution of JC-1 aggregates (Red) and JC-1 monomer (Green) cell population. Histogram calculated the relative ratio of Red against Green fluorescence (mean ± SD, n = 3). $^{*}p < 0.05$, $^{**}p < 0.01$, $^{***}p < 0.001$, NS, non-significant.

Figure S4. The overexpression of SIRT3 protects PIG3V cells against H_2O_2-induced cell apoptosis and mitochondrial dysfunction. (A) The overexpression efficiency of SIRT3 in PIG3V cells. Data represent mean ± SD (n = 3). (B) PIG3V cells transfected with plasmids OE-NC or OE-SIRT3 were treated with different concentrations of H_2O_2 (0, 0.5, 1.0 mM), and the cell viability were determined by CCK-8. Data represent mean ± SD (n = 3). (C) The apoptotic level of PIG3V cells with indicated treatment was examined by flow cytometry assay. Bar graphs represent mean ± SD (n = 3). (D) The level of apoptosis-related proteins in PIG3V cells was detected by western blotting. Data are representative of three independently experiments. (E) The ROS level of PIG3V cells was examined by MitoSOX™ Red mitochondrial superoxide indicator staining. Bar graphs represent mean ± SD (n = 3). (F) Assessment of ATP level in PIG3V cells with treatment as indicated. Data represent mean ± SD of triplicates. (G) The mitochondrial membrane potential level of PIG3V cells was examined by JC-1 staining. The scatter plot of the flow cytometry analysis shows the distribution of JC-1 aggregates (Red) and JC-1 monomer (Green) cell population. Histogram calculated the relative ratio of Red against Green fluorescence (mean ± SD, n = 3). $^{*}p < 0.05$, $^{**}p <$

0.01, $^{***}p < 0.001$, NS, non-significant.

Figure S5. The knockdown of SIRT3 has no obvious effect on the expressions of mitochondrial fussion and fission proteins. PIG1 cells were transfected with si-NC or si-SIRT3 followed by treatment with 1.0 mM H_2O_2 for 24 h.Western blotting was used to analyze protein levels of MFN1, MFN2, OPA1, DRP1and Fis1. β-Actin was detected as loading control. Data are representative of three independently performed experiments.

Figure S6. SIRT3 deficiency contributes to cell apoptosis and mitochondrial dysfunction via OPA1. (A) Representative images of apoptosis analysis by flow cytometry after indicated treatment. (B) PIG1 cells were co-transfected with si-SIRT3 and OPA1 plasmids (OE-OPA1) or control plasmids (OE-NC), and then were treated with 1.0 mM H_2O_2 for 24 h. The level of apoptosis-related proteins in PIG1 cells with indicated treatment. Data are representative of three independently experiments. Quantitative analysis on the apoptosis-related protein of interest as indicated (mean ± SD, n = 3). (C) Representative images of mitochondrial ROS analysis by flow cytometry after indicated treatment. (D) Representative images of mitochondrial membrane potential analysis by flow cytometry after indicated treatment. (E) The expressions of SIRT4 and SIRT3 in PIG1 cells with indicated treatment. Data are representative of three independently experiments. Quantitative analysis for the protein of interest as indicated (mean ± SD, n = 3). $^{**}p < 0.01$, $^{***}p < 0.001$, NS, non-significant.

Figure S7. Oxidative stress simultaneously impairs SIRT3 activity and transcription. (A) PIG1 and PIG3V cells were treated with 1.0 mM H_2O_2 for 24 h. After treatment, cells were harvested and disrupted by repeated freezing and thawing. The supernatant was further detected by the Human 4-HNE (4-Hydroxynoenal) ELISA Kit. Mean ± SD is shown (n = 3). (B) The treated cells were homogenized, and the supernatant was used for the further MDA detection by the Lipid Peroxidation MDA Assay Kit. Mean ± SD is shown (n = 3). (C) PIG1 and PIG3V cells were treated with 1.0 mM H_2O_2 for 24 h. Cell extracts were performed derivatization reaction by thawing 1× DNPH Solution, and the reaction products were further analyzed by western blotting,

β-Actin was detected as loading control. Data represent mean ± SD (n = 3). (D, E) PIG1 and PIG3V cells were transfected with si-NC or si-PGC1α. The mRNA level of SIRT3 in PIG1 and PIG3V cells was detected by RT-PCR. Data represent mean ± SD (n = 3). The protein level was detected via immunoblotting and β-Actin was detected as loading control. (F) Correlations between 8-OHdG and SIRT3 expression, 8-OHdG and PGC1α expression, and SIRT3 and PGC1α expression in melanocytes of vitiligo lesion measured via Spearman correlation (n = 8).

Figure S8. HKL protects vitiligo melanocytes against oxidative stress by activating SIRT3-OPA1 axis. (A) PIG3V cells were pre-treated with different doses of HKL as indicated, followed by exposure to 1.0 mM H_2O_2 for 24 h. CCK-8 was performed to evaluate cell ability. Data represent mean ± SD (n = 3). (B-C) PIG3V cells were pre-treated with 5 μM HKL for 24 h and then treated with 1.0 mM H_2O_2 for 24 h. The mRNA and the protein levels of PGC1α were detected by qRT-PCR and immunoblotting. Data represent mean ±SD (n = 3). (D) Enrichment of PGC1α to the promoter of SIRT3 after indicated treatment in PIG3V cells. Data are presented as mean ± SD (n = 3). (E) Representative images of apoptosis analysis by flow cytometry after indicated treatment. (F) Representative images of mitochondrial ROS analysis by flow cytometry after indicated treatment. (G) Representative images of mitochondrial membrane potential analysis by flow cytometry after indicated treatment. (H) Representative images of apoptosis analysis by flow cytometry after indicated treatment. (I) Representative images of mitochondrial ROS analysis by flow cytometry after indicated treatment. (J) Representative images of mitochondrial membrane potential analysis by flow cytometry after indicated treatment. (K) PIG3V cells were pre-treated with 5 μM HKL for 24 h and then treated with 1.0 mM H_2O_2 for 24 h. Data are representative of three independently experiments. Quantitative analysis on the expression of apoptosis-related proteins of interest as indicated.

Supplementary Figures

Figure S1

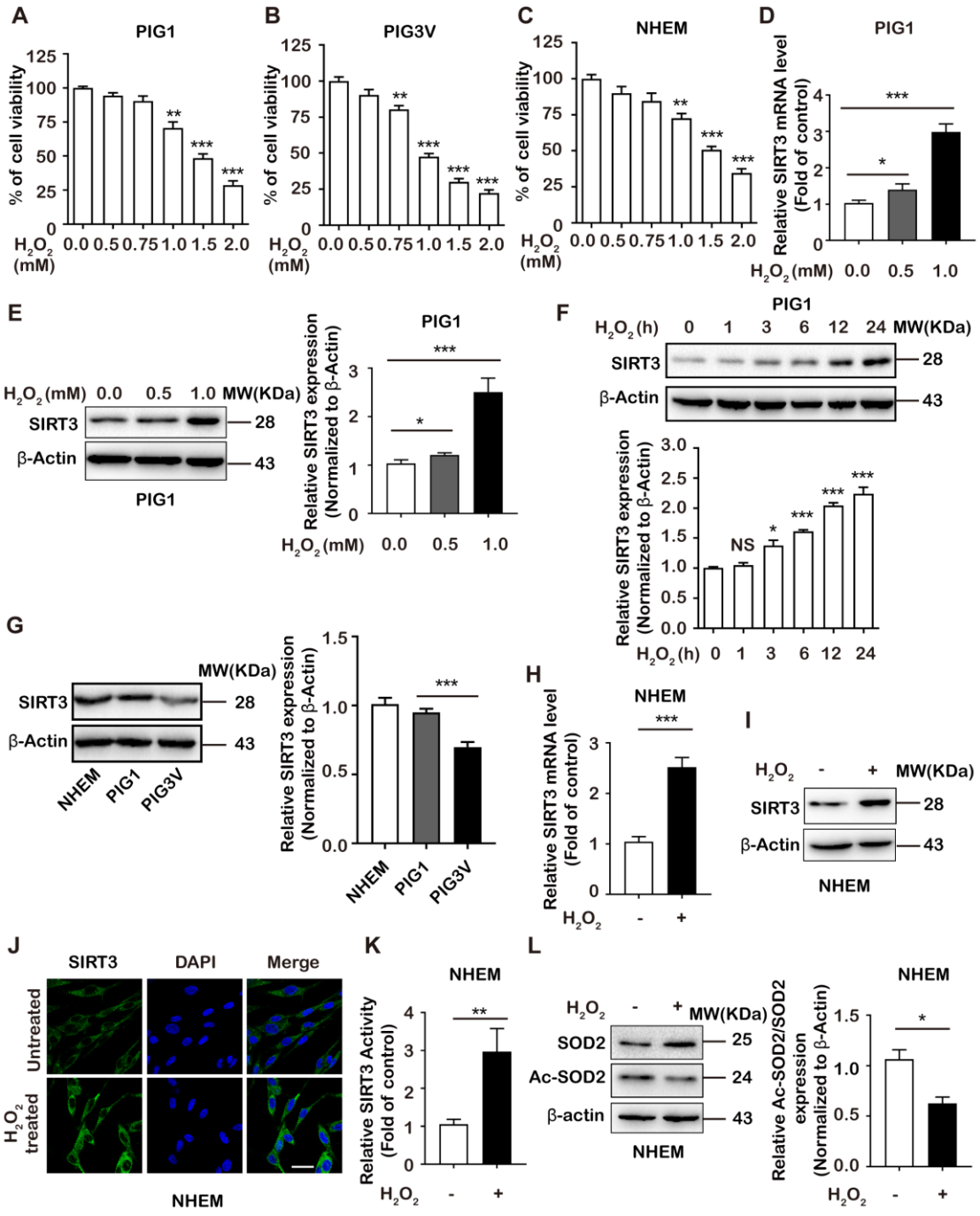

Figure S2

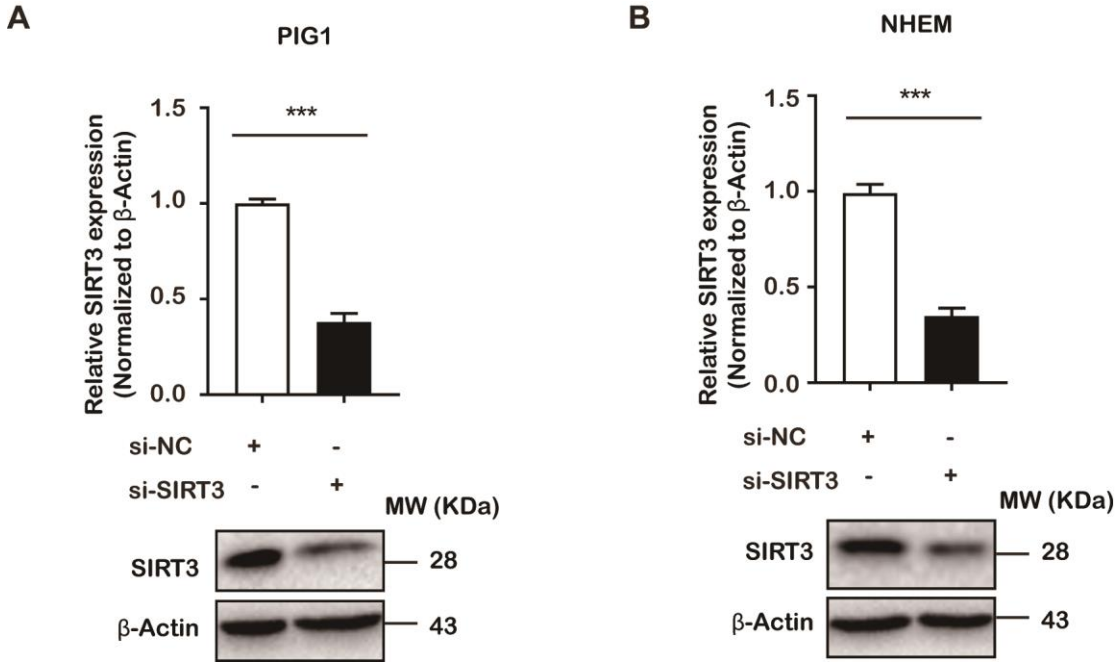
A
PIG1
Relative SIRT3 expression (Normalized to β-Actin)
1.5
1.0
0.5
0.0
***
si-NC + -
si-SIRT3 - +
MW (KDa)
SIRT3
28
β-Actin
43
B
NHEM
Relative SIRT3 expression (Normalized to β-Actin)
1.5
1.0
0.5
0.0
***
si-NC + -
si-SIRT3 - +
MW (KDa)
SIRT3
28
β-Actin
43

Figure S3

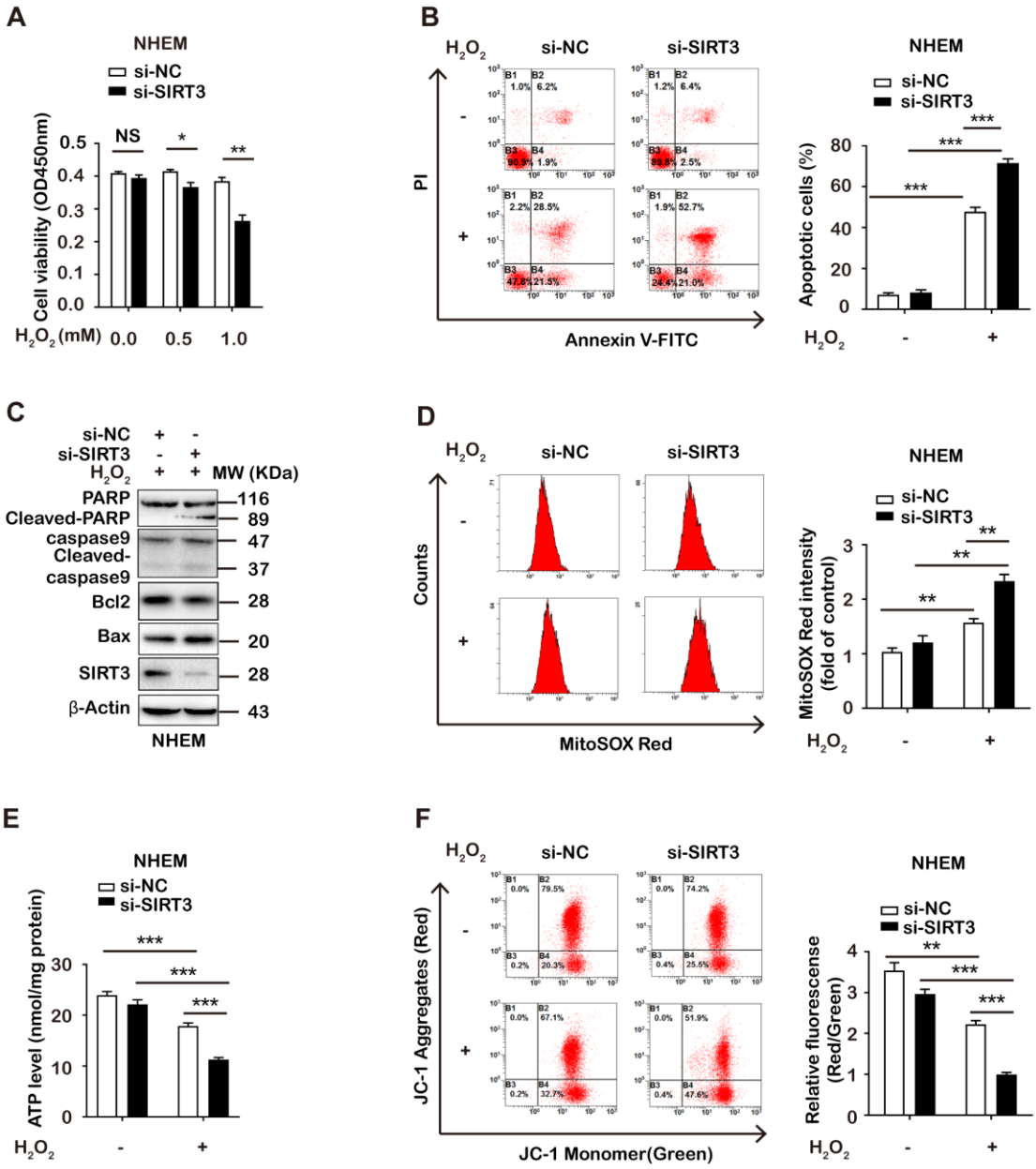
A
NHEM
si-NC
si-SIRT3
Cell viability (OD450nm)
NS
*
**
H2O2 (mM) 0.0 0.5 1.0
B
H2O2
si-NC
si-SIRT3
PI
Annexin V-FITC
NHEM
Apoptotic cells (%)
***
C
si-NC
si-SIRT3
H2O2
MW (KDa)
PARP
Cleaved-PARP
caspase9
Cleaved-caspase9
Bcl2
Bax
SIRT3
β-Actin
116
89
47
37
28
20
28
43
NHEM
D
Counts
MitoSOX Red
MitoSOX Red intensity (fold of control)
**
E
ATP level (nmol/mg protein)
F
JC-1 Aggregates (Red)
JC-1 Monomer(Green)
Relative fluorescense (Red/Green)

Figure S4

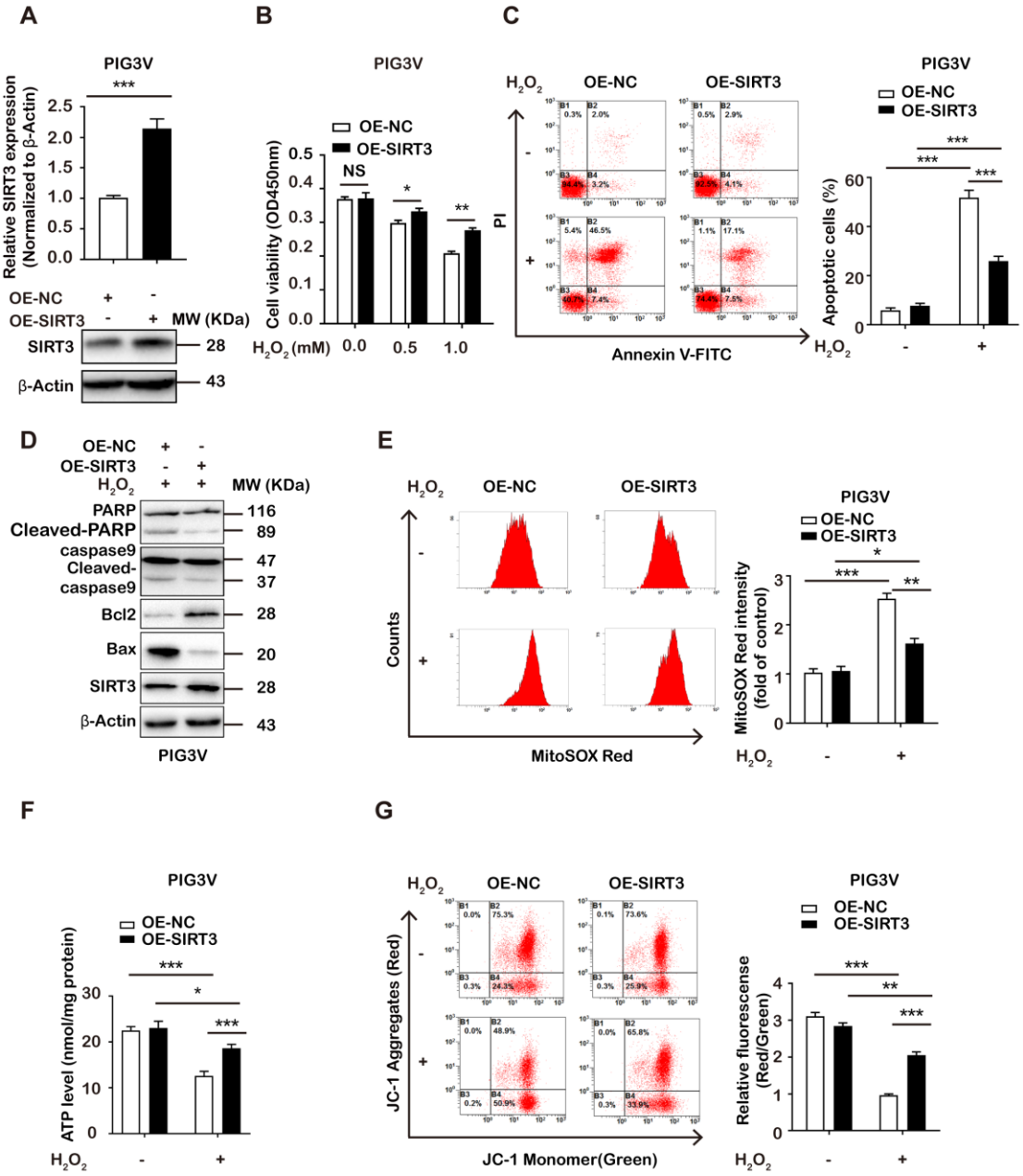
A
PIG3V
Relative SIRT3 expression (Normalized to β-Actin)
OE-NC
OE-SIRT3
MW (KDa)
SIRT3
28
β-Actin
43
B
PIG3V
OE-NC
OE-SIRT3
Cell viability (OD450nm)
NS
H2O2 (mM) 0.0 0.5 1.0
C
H2O2
OE-NC
OE-SIRT3
PI
Annexin V-FITC
PIG3V
Apoptotic cells (%)
D
PARP
Cleaved-PARP
caspase9
Cleaved-caspase9
Bcl2
Bax
SIRT3
β-Actin
PIG3V
E
Counts
MitoSOX Red
MitoSOX Red intensity (fold of control)
F
ATP level (nmol/mg protein)
G
JC-1 Aggregates (Red)
JC-1 Monomer(Green)
Relative fluorescense (Red/Green)

Figure S5

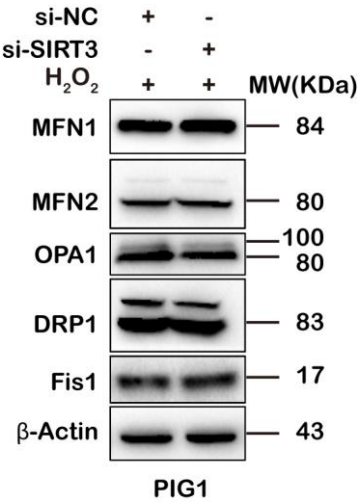
si-NC + -
si-SIRT3 - +
H2O2 + + MW(KDa)
MFN1
84
MFN2
80
OPA1
100
80
DRP1
83
Fis1
17
β-Actin
43
PIG1

Figure S6

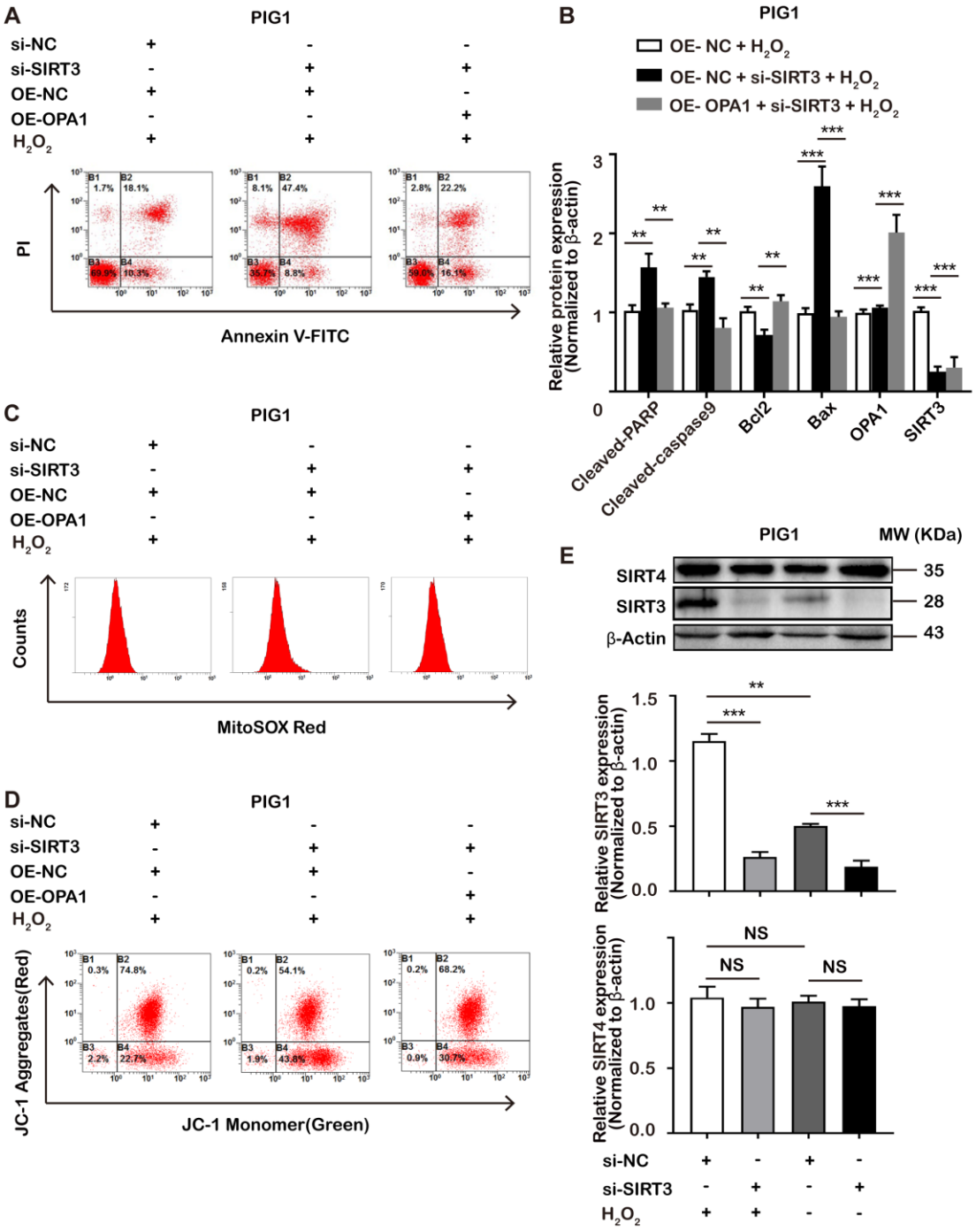
A
PIG1
si-NC + - -
si-SIRT3 - + +
OE-NC + + -
OE-OPA1 - - +
H2O2 + + +
PI
Annexin V-FITC
B
PIG1
OE- NC + H2O2
OE- NC + si-SIRT3 + H2O2
OE- OPA1 + si-SIRT3 + H2O2
Relative protein expression (Normalized to β-actin)
Cleaved-PARP
Cleaved-caspase9
Bcl2
Bax
OPA1
SIRT3
C
PIG1
si-NC + - -
si-SIRT3 - + +
OE-NC + + -
OE-OPA1 - - +
H2O2 + + +
Counts
MitoSOX Red
D
PIG1
si-NC + - -
si-SIRT3 - + +
OE-NC + + -
OE-OPA1 - - +
H2O2 + + +
JC-1 Aggregates(Red)
JC-1 Monomer(Green)
E
PIG1
MW (KDa)
SIRT4
SIRT3
β-Actin
35
28
43
Relative SIRT3 expression (Normalized to β-actin)
Relative SIRT4 expression (Normalized to β-actin)
NS
si-NC + - + -
si-SIRT3 - + - +
H2O2 + + - -

Figure S7

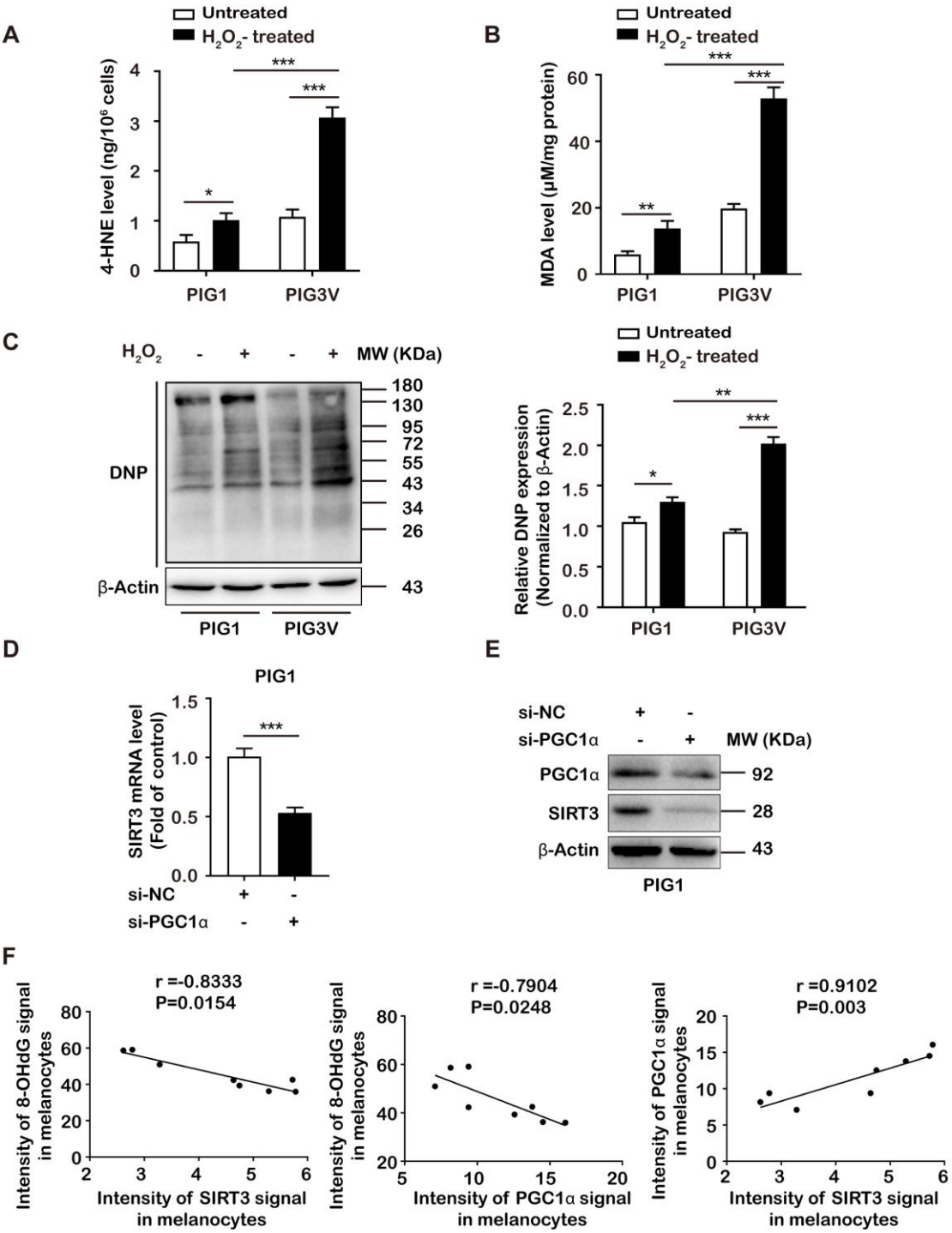
A
Untreated
H2O2- treated
4-HNE level (ng/10^6 cells)
PIG1
PIG3V
B
MDA level (μM/mg protein)
C
H2O2
MW (KDa)
DNP
β-Actin
Relative DNP expression (Normalized to β-Actin)
D
PIG1
SIRT3 mRNA level (Fold of control)
si-NC
si-PGC1α
E
PGC1α
SIRT3
F
r =-0.8333
P=0.0154
Intensity of 8-OHdG signal in melanocytes
Intensity of SIRT3 signal in melanocytes
r =-0.7904
P=0.0248
Intensity of PGC1α signal in melanocytes
r =0.9102
P=0.003

Figure S8

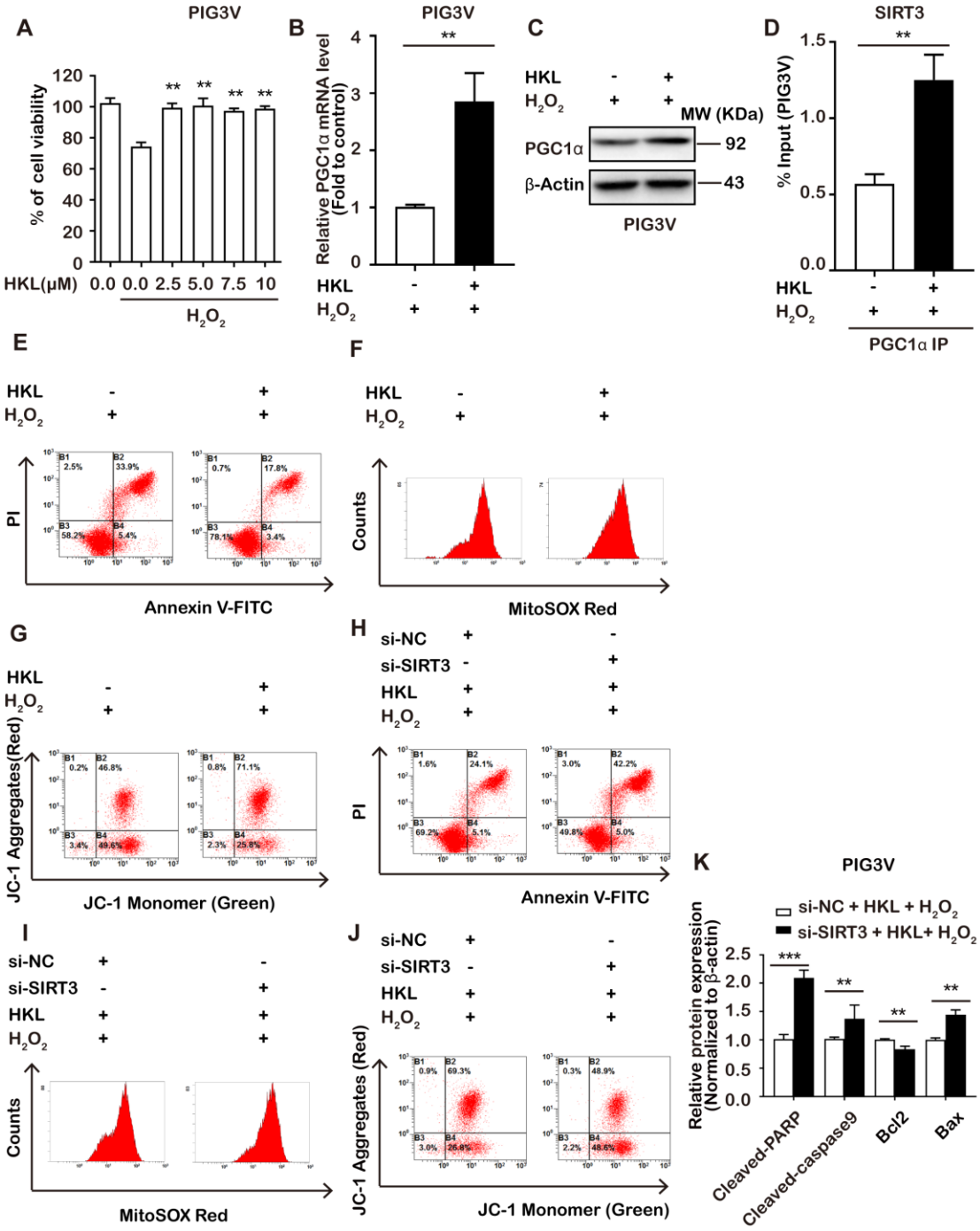
A
PIG3V
% of cell viability
HKL(μM) 0.0 0.0 2.5 5.0 7.5 10
H2O2
B
PIG3V
Relative PGC1α mRNA level (Fold to control)
HKL
H2O2
C
HKL
H2O2
MW (KDa)
PGC1α
92
β-Actin
43
PIG3V
D
SIRT3
% Input (PIG3V)
HKL
H2O2
PGC1α IP
E
HKL
H2O2
PI
Annexin V-FITC
F
HKL
H2O2
Counts
MitoSOX Red
G
HKL
H2O2
JC-1 Aggregates(Red)
JC-1 Monomer (Green)
H
si-NC
si-SIRT3
HKL
H2O2
PI
Annexin V-FITC
I
si-NC
si-SIRT3
HKL
H2O2
Counts
MitoSOX Red
J
si-NC
si-SIRT3
HKL
H2O2
JC-1 Aggregates (Red)
JC-1 Monomer (Green)
K
PIG3V
si-NC + HKL + H2O2
si-SIRT3 + HKL+ H2O2
Relative protein expression (Normalized to β-actin)
Cleaved-PARP
Cleaved-caspase9
Bcl2
Bax

Supplementary mean ± SD values of all figures

Figure 1-A:

PIG1-untreated: 1.087 ± 0.1126, n=3; PIG1-H_2O_2-treated: 2.903 ± 0.22, n=3; PIG3V-untreated: 1.043 ± 0.05364, n=3; PIG3V-H_2O_2-treated: 0.98 ± 0.05033, n=3

Figure 1-B:

PIG1-untreated: 1.077 ± 0.08686, n=3; PIG1-H_2O_2-treated: 2.046 ± 0.1135, n=3; PIG3V-untreated: 0.6338 ± 0.04574, n=3; PIG3V-H_2O_2-treated: 0.8119 ± 0.04919, n=3

Figure 1-C:

PIG1-untreated: 4.998 ± 0.2752, n=3; PIG1-H_2O_2-treated: 9.298 ± 0.7061, n=3; PIG3V-untreated: 5.235 ± 0.5315, n=3; PIG3V-H_2O_2-treated: 4.668 ± 0.4909, n=3

Figure 1-D:

PIG1-untreated: 1.057 ± 0.08838, n=3; PIG1-H_2O_2-treated: 3.733 ± 0.2028, n=3; PIG3V-untreated: 1.053 ± 0.07424, n=3; PIG3V-H_2O_2-treated: 1.087 ± 0.1186, n=3

Figure 1-E:

PIG1-untreated: 1.097 ± 0.1017, n=3; PIG1-H_2O_2-treated: 2.937 ± 0.2335, n=3; PIG3V-untreated: 1.54 ± 0.07517, n=3; PIG3V-H_2O_2-treated: 11.69 ± 0.5114, n=3

Figure 1-F:

PIG1-untreated: 1.063 ± 0.07356, n=3; PIG1-H_2O_2-treated: 0.8167 ± 0.0348, n=3; PIG3V-untreated: 1.627 ± 0.08686, n=3; PIG3V-H_2O_2-treated: 2.573 ± 0.08007, n=3

Figure 2-A:

Healthy: 14.2 ± 2.326, n=8; Vitiligo: 4.406 ± 0.4914, n=8

Figure 2-B:

Healthy: 7.675 ± 1.03, n=8; Vitiligo: 24.74 ± 1.365, n=8

Figure 3-A:

si-NC+0 mM H_2O_2: 0.3093 ± 0.005239, n=3; si-SIRT3+0 mM H_2O_2: 0.2943 ± 0.009701, n=3; si-NC+0.5 mM H_2O_2: 0.315 ± 0.005568, n=3; si-SIRT3+0.5 mM H_2O_2: 0.28 ± 0.005196, n=3

si-NC+1.0 mM H_2O_2: 0.2823 ± 0.007839, n=3; si-SIRT3+1.0 mM H_2O_2: 0.1867 ± 0.00441, n=3

Figure 3-B:

si-NC+0 mM H_2O_2: 1.35 ± 0.152, n=3; si-SIRT3+0 mM H_2O_2: 2.33 ± 0.231, n=3; si-NC+1.0 mM

H_2O_2: 30.95 ± 2.054, n=3; si-SIRT3+1.0 mM H_2O_2: 61.05 ± 2.151, n=3

Figure 3-C:

Cleaved-PARP:

si-NC+1.0 mM H_2O_2: 0.9967 ± 0.0174, n=3; si-SIRT3+1.0 mM H_2O_2: 1.469 ± 0.09911, n=3

Cleaved-caspase9:

si-NC+1.0 mM H_2O_2: 1.032 ± 0.03921, n=3; si-SIRT3+1.0 mM H_2O_2: 1.876 ± 0.05845, n=3

Bcl2:

si-NC+1.0 mM H_2O_2: 0.9917 ± 0.02489, n=3; si-SIRT3+1.0 mM H_2O_2: 0.6969 ± 0.03166, n=3

Bax:

si-NC+1.0 mM H_2O_2: 1.025 ± 0.02991, n=3; si-SIRT3+1.0 mM H_2O_2: 1.859 ± 0.08722, n=3

SIRT3:

si-NC+1.0 mM H_2O_2: 1.021 ± 0.02439, n=3; si-SIRT3+1.0 mM H_2O_2: 0.4682 ± 0.05687, n=3

Figure 3-D:

si-NC+0 mM H_2O_2: 0.9987 ± 0.0452, n=3; si-SIRT3+0 mM H_2O_2: 1.045 ± 0.05142, n=3; si-NC+1.0 mM H_2O_2: 1.657 ± 0.05852, n=3; si-SIRT3+1.0 mM H_2O_2: 2.662 ± 0.151, n=3

Figure 3-E:

si-NC+0 mM H_2O_2: 24.27 ± 0.6012, n=3; si-SIRT3+0 mM H_2O_2: 22.88 ± 0.3876, n=3

si-NC+1.0 mM H_2O_2: 17.2 ± 0.5749, n=3; si-SIRT3+1.0 mM H_2O_2: 9.584 ± 0.8315, n=3

Figure 3-F:

si-NC+0 mM H_2O_2: 5.72 ± 0.1332, n=3; si-SIRT3+0 mM H_2O_2: 5.353 ± 0.2245, n=3; si-NC+1.0 mM H_2O_2: 3.633 ± 0.2027, n=3; si-SIRT3+1.0 mM H_2O_2: 2.167 ± 0.1081, n=3

Figure 4-C:

PIG1-ComplexI:

si-NC+0 mM H_2O_2: 1.005 ± 0.03951, n=3; si-SIRT3+0 mM H_2O_2: 0.9317 ± 0.02418, n=3

si-NC+1.0 mM H_2O_2: 0.7763 ± 0.05067, n=3; si-SIRT3+1.0 mM H_2O_2: 0.3652 ± 0.07303, n=3

PIG1-ComplexII:

si-NC+0 mM H_2O_2: 1.05 ± 0.05681, n=3; si-SIRT3+0 mM H_2O_2: 0.9857 ± 0.0579, n=3; si-NC+1.0 mM H_2O_2: 0.7734 ± 0.05182, n=3; si-SIRT3+1.0 mM H_2O_2: 0.3428 ± 0.02895, n=3

PIG1-ComplexIII:

si-NC+0 mM H_2O_2: 1.001 ± 0.02593, n=3; si-SIRT3+0 mM H_2O_2: 0.8778 ± 0.04757, n=3

si-NC+1.0 mM H_2O_2: 0.7528 ± 0.02986, n=3; si-SIRT3+1.0 mM H_2O_2: 0.2556 ± 0.04619, n=3

PIG1-ComplexIV:

si-NC+0 mM H_2O_2: 1.022 ± 0.05799, n=3; si-SIRT3+0 mM H_2O_2: 0.9415 ± 0.01797, n=3; si-NC+1.0 mM H_2O_2: 0.7325 ± 0.05822, n=3; si-SIRT3+1.0 mM H_2O_2: 0.4028 ± 0.01357, n=3

PIG1-ComplexV:

si-NC+0 mM H_2O_2: 1.012 ± 0.03424, n=3; si-SIRT3+0 mM H_2O_2: 0.9143 ± 0.01062, n=3

si-NC+1.0 mM H_2O_2: 0.5616 ± 0.03702, n=3; si-SIRT3+1.0 mM H_2O_2: 0.1905 ± 0.01238, n=3

PIG3V-ComplexI:

OE-NC+0 mM H_2O_2: 1.035 ± 0.04585, n=3; OE-SIRT3+0 mM H_2O_2: 1.065 ± 0.04087, n=3

OE-NC+1.0 mM H_2O_2: 0.5987 ± 0.02068, n=3; OE-SIRT3+1.0 mM H_2O_2: 0.9253 ± 0.01615, n=3

PIG3V-ComplexII:

OE-NC+0 mM H_2O_2: 0.9899 ± 0.0284, n=3; OE-SIRT3+0 mM H_2O_2: 1.086 ± 0.0579, n=3

OE-NC+1.0 mM H_2O_2: 0.6076 ± 0.03639, n=3; OE-SIRT3+1.0 mM H_2O_2: 0.8562 ± 0.01152, n=3

PIG3V-ComplexIII:

OE-NC+0 mM H_2O_2: 1.018 ± 0.05265, n=3; OE-SIRT3+0 mM H_2O_2: 1.031 ± 0.06992, n=3

OE-NC+1.0 mM H_2O_2: 0.5109 ± 0.0306, n=3; OE-SIRT3+1.0 mM H_2O_2: 0.9353 ± 0.02649, n=3

PIG3V-ComplexIV:

OE-NC+0 mM H_2O_2: 0.979 ± 0.03266, n=3; OE-SIRT3+0 mM H_2O_2: 1.021 ± 0.01536, n=3

OE-NC+1.0 mM H_2O_2: 0.5557 ± 0.03253, n=3; OE-SIRT3+1.0 mM H_2O_2: 0.8861 ± 0.02248, n=3

PIG3V-ComplexV:

OE-NC+0 mM H_2O_2: 1.025 ± 0.047, n=3; OE-SIRT3+0 mM H_2O_2: 1.061 ± 0.07182, n=3

OE-NC+1.0 mM H_2O_2: 0.3777 ± 0.02464, n=3; OE-SIRT3+1.0 mM H_2O_2: 0.8505 ± 0.0205, n=3

Figure 4-D:

PIG1:

si-NC+1.0 mM H_2O_2: n=100

Fragmented: 22.33 ± 1.856; Intermediate: 44.67 ± 2.906; Tubulated: 33 ± 2.082

si-SIRT3+1.0 mM H_2O_2: n=100

Fragmented: 55 ± 3.606; Intermediate: 27 ± 2.309; Tubulated: 18 ± 1.528

PIG3V:

OE-NC+1.0 mM H_2O_2: n=100

Fragmented: 52.33 ± 1.856; Intermediate: 31.33 ± 1.333; Tubulated: 16.33 ± 1.453

OE-SIRT3+1.0 mM H_2O_2: n=100

Fragmented: 25 ± 2.517; Intermediate: 47 ± 3.464; Tubulated: 28 ± 1.528

Figure 4-E:

PIG1:

si-NC+0 mM H_2O_2: 1.145 ± 0.162, n=100; si-NC+1.0 mM H_2O_2: 0.7341 ± 0.09165, n=100; si-SIRT3+1.0 mM H_2O_2: 0.4287 ± 0.05984, n=100

PIG3V:

OE-NC+0 mM H_2O_2: 0.8567 ± 0.1642, n=100; OE-NC+1.0 mM H_2O_2: 0.4598 ± 0.07502, n=100

OE-SIRT3+1.0 mM H_2O_2: 0.8196 ± 0.1465, n=100

Figure 5-B:

PIG1:

OE-NC+1.0 mM H_2O_2: n=100

Fragmented: 25.67 ± 2.603; Intermediate: 46.67 ± 1.764; Tubulated: 30.33 ± 2.603

si-SIRT3+ OE-NC+1.0 mM H_2O_2: n=100

Fragmented: 51.67 ± 2.728; Intermediate: 30.33 ± 1.764; Tubulated: 18 ± 1.528

si-SIRT3+ OE-OPA1+1.0 mM H_2O_2: n=100

Fragmented: 23.67 ± 0.6667; Intermediate: 43 ± 1.155; Tubulated: 33.33 ± 1.764

Figure 5-D:

PIG1-ComplexI:

OE-NC+1.0 mM H_2O_2: 1.051 ± 0.06306, n=3; si-SIRT3+ OE-NC+1.0 mM H_2O_2: 0.5322 ± 0.06173, n=3; si-SIRT3+ OE-OPA1+1.0 mM H_2O_2: 0.8322 ± 0.01268, n=3

PIG1-ComplexII:

OE-NC+1.0 mM H_2O_2: 0.9999 ± 0.04238, n=3; si-SIRT3+ OE-NC+1.0 mM H_2O_2: 0.4628 ± 0.04014, n=3; si-SIRT3+ OE-OPA1+1.0 mM H_2O_2: 0.7628 ± 0.04014, n=3

PIG1-ComplexIII:

OE-NC+1.0 mM H_2O_2: 1.064 ± 0.09232, n=3; si-SIRT3+ OE-NC+1.0 mM H_2O_2: 0.4089 ± 0.02339,

n=3; si-SIRT3+ OE-OPA1+1.0 mM H_2O_2: 0.7756 ± 0.02117, n=3

PIG1-ComplexIV:

OE-NC+1.0 mM H_2O_2: 0.9824 ± 0.03494, n=3; si-SIRT3+ OE-NC+1.0 mM H_2O_2: 0.5461 ± 0.01661, n=3; si-SIRT3+ OE-OPA1+1.0 mM H_2O_2: 0.8461 ± 0.01661, n=3

PIG1-ComplexV:

OE-NC+1.0 mM H_2O_2: 1.062 ± 0.06727, n=3; si-SIRT3+ OE-NC+1.0 mM H_2O_2: 0.3438 ± 0.02772, n=3; si-SIRT3+ OE-OPA1+1.0 mM H_2O_2: 0.7438 ± 0.02772, n=3

Figure 5-E:

PIG1:

OE-NC+1.0 mM H_2O_2: 28.4 ± 2.252, n=3; si-SIRT3+ OE-NC+1.0 mM H_2O_2: 55.53 ± 2.963, n=3; si-SIRT3+ OE-OPA1+1.0 mM H_2O_2: 38 ± 1.48, n=3

Figure 5-G:

PIG1:

OE-NC+1.0 mM H_2O_2: 1.028 ± 0.04081, n=3; si-SIRT3+ OE-NC+1.0 mM H_2O_2: 1.513 ± 0.02728, n=3; si-SIRT3+ OE-OPA1+1.0 mM H_2O_2: 1.1 ± 0.03606, n=3

Figure 5-H:

PIG1:

OE-NC+1.0 mM H_2O_2: 3 ± 0.1528, n=3; si-SIRT3+ OE-NC+1.0 mM H_2O_2: 1.147 ± 0.0491, n=3; si-SIRT3+ OE-OPA1+1.0 mM H_2O_2: 2.427 ± 0.1035, n=3

Figure 5-I:

PIG1:

OE-NC+1.0 mM H_2O_2: 18.13 ± 0.5085, n=3; si-SIRT3+ OE-NC+1.0 mM H_2O_2: 10.47 ± 0.472, n=3; si-SIRT3+ OE-OPA1+1.0 mM H_2O_2: 15.23 ± 0.1941, n=3

Figure 6-A:

Healthy: 17.29 ± 2.18, n=8; Vitiligo: 34.48 ± 3.445, n=8

Figure 6-B:

PIG1-untreated: 1.01 ± 0.02082, n=3; PIG1-H_2O_2-treated: 0.8067 ± 0.02333, n=3; PIG3V-untreated: 0.8367 ± 0.0318, n=3; PIG3V-H_2O_2-treated: 1.68 ± 0.09018, n=3

Figure 6-C:

PIG1-untreated: 1.047 ± 0.06227, n=3; PIG1-H_2O_2-treated: 2.65 ± 0.07211, n=3; PIG3V-untreated: 1.057 ± 0.0348, n=3; PIG3V-H_2O_2-treated: 1.267 ± 0.1885, n=3

Figure 6-D:

PIG1-untreated: 1.043 ± 0.04842, n=3; PIG1-H_2O_2-treated: 1.607 ± 0.07881, n=3; PIG3V-untreated: 0.68 ± 0.02646, n=3; PIG3V-H_2O_2-treated: 0.7533 ± 0.01764, n=3

Figure 6-E:

PIG1-untreated: 0.8133 ± 0.0491, n=3; PIG1-H_2O_2-treated: 1.617 ± 0.09821, n=3; PIG3V-untreated: 0.7267 ± 0.07535, n=3; PIG3V-H_2O_2-treated: 0.6733 ± 0.08647, n=3

Figure 6-F:

Healthy: 25.66 ± 1.843, n=8; Vitiligo: 12.03 ± 1.382, n=8

Figure 7-A:

5 μM HKL+0 mM H_2O_2: 1.047 ± 0.08969, n=3; 5 μM HKL+1.0 mM H_2O_2: 2.23 ± 0.1644, n=3

Figure 7-C:

5 μM HKL+0 mM H_2O_2: 1.02 ± 0.1159, n=3; 5 μM HKL+1.0 mM H_2O_2: 3.697 ± 0.4659, n=3

Figure 7-D:

5 μM HKL+0 mM H_2O_2: 1.017 ± 0.0441, n=3; 5 μM HKL+1.0 mM H_2O_2: 0.4193 ± 0.06822, n=3

Figure 7-E:

5 μM HKL+0 mM H_2O_2: n=100

Fragmented: 59 ± 2.517, n=3; Intermediate: 31.67 ± 2.404, n=3; Tubulated: 9.333 ± 0.8819, n=3

5 μM HKL+1.0 mM H_2O_2: n=100

Fragmented: 22 ± 1.528, n=3; Intermediate: 45.67 ± 2.603, n=3; Tubulated: 30.67 ± 2.848, n=3

Figure 7-F:

PIG3V-apoptotic:

5 μM HKL+0 mM H_2O_2: 39.17 ± 1.387, n=3; 5 μM HKL+1.0 mM H_2O_2: 19.63 ± 2.521, n=3

PIG3V-mitochondrial ROS:

5 μM HKL+0 mM H_2O_2: 1.047 ± 0.08969, n=3; 5 μM HKL+1.0 mM H_2O_2: 0.703 ± 0.01328, n=3

PIG3V-mitochondrial membrane potential:

5 μM HKL+0 mM H_2O_2: 0.98 ± 0.1172, n=3; 5 μM HKL+1.0 mM H_2O_2: 2.92 ± 0.2996, n=3

PIG3V-ATP

5 μM HKL+0 mM H_2O_2: 10.75 ± 0.4579, n=3; 5 μM HKL+1.0 mM H_2O_2: 16.91 ± 0.3243, n=3

Figure 7-G:

PIG3V:

si-NC+5 μM HKL+1.0 mM H_2O_2: n=100

Fragmented: 23 ± 2.082, n=3; Intermediate: 45.33 ± 2.186, n=3; Tubulated: 31.67 ± 1.856, n=3

si-OPA1+5 μM HKL+1.0 mM H_2O_2: n=100

Fragmented: 54.67 ± 2.728, n=3; Intermediate: 31.33 ± 1.856, n=3; Tubulated: 14 ± 1.732, n=3

Figure 7-H:

PIG3V-apoptotic:

si-NC+5 μM HKL+1.0 mM H_2O_2: 26.93 ± 1.8, n=3; si-OPA1+5 μM HKL+1.0 mM H_2O_2: 47.97 ± 2.484, n=3

PIG3V-mitochondrial ROS:

si-NC+5 μM HKL+1.0 mM H_2O_2: 1.004 ± 0.02233, n=3; si-OPA1+5 μM HKL+1.0 mM H_2O_2: 1.327 ± 0.04978, n=3

PIG3V-mitochondrial membrane potential:

si-NC+5 μM HKL+1.0 mM H_2O_2: 2.97 ± 0.2234, n=3; si-OPA1+5 μM HKL+1.0 mM H_2O_2: 1.037 ± 0.09135, n=3

PIG3V-ATP

si-NC+5 μM HKL+1.0 mM H_2O_2: 18.08 ± 0.4444, n=3; si-OPA1+5 μM HKL+1.0 mM H_2O_2: 11.61 ± 0.3332, n=3

Figure 7-K:

PIG3V-ComplexI:

si-NC+5 μM HKL+1.0 mM H_2O_2: 1.009 ± 0.03117, n=3; si-OPA1+5 μM HKL+1.0 mM H_2O_2: 0.5122 ± 0.04248, n=3

PIG3V-ComplexII:

si-NC+5 μM HKL+1.0 mM H_2O_2: 1.027 ± 0.05546, n=3; si-OPA1+5 μM HKL+1.0 mM H_2O_2: 0.5928 ± 0.02895, n=3

PIG3V-ComplexIII:

si-NC+5 μM HKL+1.0 mM H_2O_2: 1.008 ± 0.02624, n=3; si-OPA1+5 μM HKL+1.0 mM H_2O_2:

0.3989 ± 0.01833, n=3

PIG3V-ComplexIV:

si-NC+5 μM HKL+1.0 mM H_2O_2: 0.9924 ± 0.02544, n=3; si-OPA1+5 μM HKL+1.0 mM H_2O_2: 0.5128 ± 0.02453, n=3

PIG3V-ComplexV:

si-NC+5 μM HKL+1.0 mM H_2O_2: 1.009 ± 0.03685, n=3; si-OPA1+5 μM HKL+1.0 mM H_2O_2: 0.4171 ± 0.026, n=3

Figure S1-A:

PIG1:

0 mM H_2O_2 treated: 100 ± 1.155, n=3; 0.5 mM H_2O_2 treated: 94.33 ± 2.186, n=3; 0.75 mM H_2O_2 treated: 89.67 ± 3.844, n=3; 1.0 mM H_2O_2 treated: 70.67 ± 4.41, n=3; 1.5 mM H_2O_2 treated: 48.33 ± 3.283, n=3; 2.0 mM H_2O_2 treated: 28.67 ± 3.18, n=3

Figure S1-B:

PIG3V:

0 mM H_2O_2 treated: 100 ± 2.887, n=3; 0.5 mM H_2O_2 treated: 90.33 ± 3.756, n=3; 0.75 mM H_2O_2 treated: 80.33 ± 2.603, n=3; 1.0 mM H_2O_2 treated: 47.67 ± 2.028, n=3; 1.5 mM H_2O_2 treated: 30.04 ± 2.309, n=3; 2.0 mM H_2O_2 treated: 22.33 ± 2.186, n=3

Figure S1-C:

NHEM:

0 mM H_2O_2 treated: 100 ± 2.887, n=3; 0.5 mM H_2O_2 treated: 90.03 ± 4.619, n=3; 0.75 mM H_2O_2 treated: 84.67 ± 5.364, n=3; 1.0 mM H_2O_2 treated: 72.67 ± 3.18, n=3; 1.5 mM H_2O_2 treated: 50.67 ± 2.404, n=3; 2.0 mM H_2O_2 treated: 34.67 ± 2.848, n=3

Figure S1-D:

PIG1-untreated: 1.03 ± 0.04604, n=3; PIG1-0.5 mM H_2O_2-treated: 1.21 ± 0.02517, n=3; PIG1-1.0 mM H_2O_2-treated: 2.51 ± 0.1652, n=3

Figure S1-E:

PIG1-untreated: 1.036 ± 0.04195, n=3; PIG1-0.5 mM H_2O_2-treated: 1.397 ± 0.09387, n=3; PIG1-1.0 mM H_2O_2-treated: 2.987 ± 0.1271, n=3

Figure S1-F:

PIG1-untreated: 1.007 ± 0.01764, n=3; PIG1-1.0 mM H_2O_2-treated for 1h: 1.05 ± 0.04022, n=3; PIG1-1.0 mM H_2O_2-treated for 3h: 1.379 ± 0.08661, n=3; PIG1-1.0 mM H_2O_2-treated for 6h: 1.616 ± 0.02602, n=3; PIG1-1.0 mM H_2O_2-treated for 12h: 2.043 ± 0.04933, n=3; PIG1-1.0 mM H_2O_2-treated for 24h: 2.24 ± 0.1097, n=3

Figure S1-G:

NHEM: 1.01 ± 0.02646, n=3; PIG1: 0.9516 ± 0.01482, n=3; PIG3V: 0.6993 ± 0.0203, n=3

Figure S1-H:

NHEM-untreated: 1.043 ± 0.05897, n=3; NHEM-H_2O_2-treated: 2.522 ± 0.1099, n=3

Figure S1-K:

NHEM-untreated: 1.053 ± 0.07424, n=3; NHEM-H_2O_2-treated: 2.967 ± 0.3528, n=3

Figure S1-L:

NHEM-untreated: 1.065 ± 0.065, n=3; NHEM-H_2O_2-treated: 0.625 ± 0.045, n=3

Figure S2-A:

si-NC: 1.001 ± 0.01272, n=3; si-SIRT3: 0.4467 ± 0.02185, n=3

Figure S2-B:

si-NC: 0.9907 ± 0.02696, n=3; si-SIRT3: 0.3478 ± 0.02386, n=3

Figure S3-A:

si-NC+0 mM H_2O_2: 0.4093 ± 0.005241, n=3; si-SIRT3+0 mM H_2O_2: 0.3943 ± 0.009812, n=3; si-NC+0.5 mM H_2O_2: 0.415 ± 0.005608, n=3; si-SIRT3+0.5 mM H_2O_2: 0.3667 ± 0.01431, n=3

si-NC+1.0 mM H_2O_2: 0.3857 ± 0.01087, n=3; si-SIRT3+1.0 mM H_2O_2: 0.2637 ± 0.01785, n=3

Figure S3-B:

si-NC+0 mM H_2O_2: 7.21 ± 0.903, n=3; si-SIRT3+0 mM H_2O_2: 7.83 ± 1.121, n=2; si-NC+1.0 mM H_2O_2: 47.95 ± 2.054, n=3; si-SIRT3+1.0 mM H_2O_2: 72.5 ± 1.221, n=3

Figure S3-D:

si-NC+0 mM H_2O_2: 1.035 ± 0.07334, n=3; si-SIRT3+0 mM H_2O_2: 1.207 ± 0.1237, n=3; si-NC+1.0 mM H_2O_2: 1.573 ± 0.07074, n=3; si-SIRT3+1.0 mM H_2O_2: 2.337 ± 0.1189, n=3

Figure S3-E:

si-NC+0 mM H_2O_2: 23.94 ± 0.4145, n=3; si-SIRT3+0 mM H_2O_2: 22.11 ± 0.536, n=3; si-NC+1.0 mM H_2O_2: 17.86 ± 0.3544, n=3; si-SIRT3+1.0 mM H_2O_2: 11.25 ± 0.2462, n=3

Figure S3-F:

si-NC+0 mM H_2O_2: 3.537 ± 0.1943, n=3; si-SIRT3+0 mM H_2O_2: 2.967 ± 0.1161, n=3; si-NC+1.0 mM H_2O_2: 2.22 ± 0.09539, n=3; si-SIRT3+1.0 mM H_2O_2: 0.99 ± 0.05508, n=3

Figure S4-A:

OE-NC: 1.01 ± 0.02082, n=3; OE-SIRT3: 2.142 ± 0.09148, n=3

Figure S4-B:

OE-NC+0 mM H_2O_2: 0.3693 ± 0.006888, n=3, n=3; OE-SIRT3+0 mM H_2O_2: 0.371 ± 0.01721, n=3; OE-NC+0.5 mM H_2O_2: 0.2983 ± 0.008293, n=3; OE-SIRT3+0.5 mM H_2O_2: 0.3333 ± 0.008647, n=3; OE-NC+1.0 mM H_2O_2: 0.209 ± 0.005508, n=3; OE-SIRT3+1.0 mM H_2O_2: 0.277 ± 0.006658, n=3

Figure S4-C:

OE-NC+0 mM H_2O_2: 6.367 ± 0.6173, n=3; OE-SIRT3+0 mM H_2O_2: 7.967 ± 0.4842, n=3; OE-NC+1.0 mM H_2O_2: 51.2 ± 1.358, n=3; OE-SIRT3+1.0 mM H_2O_2: 26.7 ± 1.082, n=3

Figure S4-E:

OE-NC+0 mM H_2O_2: 1.027 ± 0.07986, n=3; OE-SIRT3+0 mM H_2O_2: 1.062 ± 0.09482, n=3; OE-NC+1.0 mM H_2O_2: 2.536 ± 0.1105, n=3; OE-SIRT3+1.0 mM H_2O_2: 1.623 ± 0.1027, n=3

Figure S4-F:

OE-NC+0 mM H_2O_2: 22.51 ± 0.4918, n=3; OE-SIRT3+0 mM H_2O_2: 23.08 ± 0.8399, n=3; OE-NC+1.0 mM H_2O_2: 12.58 ± 0.5783, n=3; OE-SIRT3+1.0 mM H_2O_2: 18.65 ± 0.4782, n=3

Figure S4-G:

OE-NC+0 mM H_2O_2: 3.11 ± 0.1012, n=3; OE-SIRT3+0 mM H_2O_2: 2.843 ± 0.08373, n=3; OE-NC+1.0 mM H_2O_2: 0.9633 ± 0.03756, n=3; OE-SIRT3+1.0 mM H_2O_2: 2.05 ± 0.09074, n=3

Figure S6-B:

PIG1-cleaved PRAP:

OE-NC+1.0 mM H_2O_2: 1.018 ± 0.04197, n=3; si-SIRT3+ OE-NC+1.0 mM H_2O_2: 1.571 ± 0.1002, n=3; si-SIRT3+ OE-OPA1+1.0 mM H_2O_2: 1.058 ± 0.03253, n=3

PIG1-cleaved caspase9:

OE-NC+1.0 mM H_2O_2: 1.029 ± 0.04191, n=3; si-SIRT3+ OE-NC+1.0 mM H_2O_2: 1.449 ± 0.04151, n=3; si-SIRT3+ OE-OPA1+1.0 mM H_2O_2: 0.8056 ± 0.0695, n=3

PIG1-Bcl2:

OE-NC+1.0 mM H_2O_2: 1.015 ± 0.03235, n=3; si-SIRT3+ OE-NC+1.0 mM H_2O_2: 0.7139 ± 0.03885, n=3; si-SIRT3+ OE-OPA1+1.0 mM H_2O_2: 1.141 ± 0.04475, n=3

PIG1-Bax:

OE-NC+1.0 mM H_2O_2: 0.9903 ± 0.03641, n=3; si-SIRT3+ OE-NC+1.0 mM H_2O_2: 2.598 ± 0.1445, n=3; si-SIRT3+ OE-OPA1+1.0 mM H_2O_2: 0.9427 ± 0.04147, n=3

PIG1-OPA1:

OE-NC+1.0 mM H_2O_2: 0.9967 ± 0.02258, n=3; si-SIRT3+ OE-NC+1.0 mM H_2O_2: 1.06 ± 0.01516, n=3; si-SIRT3+ OE-OPA1+1.0 mM H_2O_2: 2.012 ± 0.1301, n=3

PIG1-SIRT3:

OE-NC+1.0 mM H_2O_2: 1.018 ± 0.02641, n=3; si-SIRT3+ OE-NC+1.0 mM H_2O_2: 0.2486 ± 0.03704, n=3; si-SIRT3+ OE-OPA1+1.0 mM H_2O_2: 0.3015 ± 0.07621, n=3

Figure S6-E:

PIG1-SIRT3:

si-NC+1.0 mM H_2O_2: 2.308 ± 0.06268, n=3; si-SIRT3+1.0 mM H_2O_2: 0.5277 ± 0.04387, n=3; si-NC+0 mM H_2O_2: 1.007 ± 0.01764, n=3; si-SIRT3+0 mM H_2O_2: 0.3774 ± 0.05423, n=3

PIG1-SIRT4:

si-NC+1.0 mM H_2O_2: 1.041 ± 0.04865, n=3; si-SIRT3+1.0 mM H_2O_2: 0.9692 ± 0.0366, n=3; si-NC+0 mM H_2O_2: 1.01 ± 0.02646, n=3; si-SIRT3+0 mM H_2O_2: 0.9752 ± 0.03025, n=3

Figure S7-A:

PIG1-untreated: 0.5867 ± 0.07535, n=3; PIG1-H_2O_2-treated: 1.01 ± 0.08327, n=3; PIG3V-untreated: 1.083 ± 0.08413, n=3; PIG3V-H_2O_2-treated: 3.073 ± 0.1178, n=3

Figure S7-B:

PIG1-untreated: 6.033 ± 0.4978, n=3; PIG1-H_2O_2-treated: 13.73 ± 1.338, n=3; PIG3V-untreated: 19.77 ± 0.8007, n=3; PIG3V-H_2O_2-treated: 52.83 ± 1.947, n=3

Figure S7-C:

PIG1-untreated: 1.053 ± 0.0584, n=3; PIG1-H_2O_2-treated: 1.3 ± 0.05686, n=3; PIG3V-untreated: 0.9297 ± 0.03183, n=3; PIG3V-H_2O_2-treated: 2.02 ± 0.08083, n=3

Figure S7-D:

PIG1-si-NC: 1.007 ± 0.04055, n=3; PIG1-si-PGC1α: 0.5317 ± 0.02619, n=3

Figure S8-A:

0μM HKL + 0 mM H_2O_2 treated: 102.5 ± 3.256, n=3; 0μM HKL + 1.0 mM H_2O_2 treated: 74.47 ± 2.664, n=3; 2.5μM HKL + 1.0 mM H_2O_2 treated: 99.53 ± 2.8, n=3; 5.0μM HKL + 1.0 mM H_2O_2 treated: 101 ± 4.566, n=3; 7.5μM HKL + 1.0 mM H_2O_2 treated: 97.47 ± 1.693, n=3; 10.0μM HKL + 1.0 mM H_2O_2 treated: 98.97 ± 1.594, n=3

Figure S8-B:

5 μM HKL+0 mM H_2O_2: 1.01 ± 0.02082, n=3; 5 μM HKL+1.0 mM H_2O_2: 2.857 ± 0.287, n=3

Figure S8-D:

5 μM HKL+0 mM H_2O_2: 0.57 ± 0.03606, n=3; 5 μM HKL+1.0 mM H_2O_2: 1.252 ± 0.09515, n=3

Figure S8-K:

Cleaved-PARP:

si-NC+5 μM HKL+1.0 mM H_2O_2: 1.011 ± 0.04764, n=3; si-OPA1+5 μM HKL+1.0 mM H_2O_2: 2.092 ± 0.08015, n=3

Cleaved-caspase9:

si-NC+5 μM HKL+1.0 mM H_2O_2: 1.017 ± 0.01768, n=3; si-OPA1+5 μM HKL+1.0 mM H_2O_2: 1.372 ± 0.1388, n=3

Bcl2:

si-NC+5 μM HKL+1.0 mM H_2O_2: 1.003 ± 0.009905, n=3; si-OPA1+5 μM HKL+1.0 mM H_2O_2: 0.8322 ± 0.0327, n=3

Bax:

si-NC+5 μM HKL+1.0 mM H_2O_2: 1 ± 0.01934, n=3; si-OPA1+5 μM HKL+1.0 mM H_2O_2: 1.443 ± 0.04936, n=3